

# MASS TRANSFER FROM DROPLETS FALLING THROUGH A QUIESCENT BATH

BY  
UDAY CHATTERJEE

511

ME

1971

M

CHA

THA



DEPARTMENT OF METALLURGICAL ENGINEERING  
INDIAN INSTITUTE OF TECHNOLOGY KANPUR  
JUNE 1971

CENTRAL LIBRARY  
Indian Institute of Technology  
KANPUR

Class No. ~~7A636~~.....  
~~669.73~~  
C 352

# MASS TRANSFER FROM DROPLETS FALLING THROUGH A QUIESCENT BATH

A Thesis Submitted  
In Partial Fulfillment of the Requirements  
for the Degree of  
MASTER OF TECHNOLOGY

BY  
LOAY CHATTERJEE



511

on 12/6

DEPARTMENT OF METALLURGICAL ENGINEERING  
INDIAN INSTITUTE OF TECHNOLOGY KANPUR  
JUNE 1971

ME - 1971 - M - CHA - MAS



~~CONFIDENTIAL~~

This is to certify that the study of  
"Mass transfer from droplets falling through a quiescent  
liquid" has been carried out by DR. UDAY CHATTERJEE  
under my supervision and that this work has not been  
submitted elsewhere for a degree.

*Alakh*

(Dr. UDAY)

ASSISTANT PROFESSOR

SCHOOL OF CHEMICAL ENGINEERING

Indian Institute of Technology Kanpur



## ABSTRACT

Transfer of indium from falling mercury-indium amalgam droplets to a static bath of aqueous ferric chloride solution was investigated at 25°C. The viscosity of the aqueous solution was varied by addition of glycerol up to 46 percent. The reaction was:



Two droplet sizes were employed. The change of concentration of  $In^{3+}$  in the aqueous phase as a function of time was followed by sampling and polarographic analysis. The diffusion coefficient of ferric ion at various concentrations were measured by polarographic technique. The terminal velocity and residence times of the droplets were measured by photographic technique. Efforts were also made to get an idea of the droplet oscillation during their fall through aqueous phase. Kinetic considerations and mass-transfer calculations confirm aqueous control. However,  $\log \frac{[Fe^{3+}]_0}{[Fe^{3+}]_t}$  show some unexpected deviation from linearity when plotted against time. Variation of diffusion coefficient with concentration of ferric ion does not explain this departure from linearity completely. The drag coefficient vs Reynold's number behaviour is very close to that obtained by Calderbank et al and shows departure from solid sphere behaviour at high Reynold's number. The mass-transfer coefficient is one order magnitude higher than that expected from the solid sphere behaviour presumably due to droplet oscillation and possibly Marangoni effect. The droplets attained terminal velocity at a very short distance after the fall.

It has been a great pleasure to work on the present problem concerning the most important but hitherto overlooked aspect of desulfurization in blast furnaces. I am thankful to Dr. A. Chouk and Dr. A.M. Shams for selecting this important and sensitive problem of today, and their constant aid and determination to meet the challenges encountered in successful completion of the work.

I am grateful to Dr. A.M. Sogah for providing high purity sulfur for nontransfer study.

I am thankful to Dr. A.M. Elghay for extending all facilities for using the Polarograph, and to Mr. Jeyarajah who trained me in handling the instrument.

I gratefully acknowledge Dr. F.M. Elmaghrabi's help in selecting the separating liquid used in the bath.

Dr. A.M. Shams's guidance in measuring terminal velocity of droplets by electrical techniques is sincerely acknowledged.

Mrs. A.M. Elgadi and Mr. F. Elmaghrabi both Graduate students deserve my sincere thanks for their help in doing the photographic work. I am grateful to Mr. A. Sam and A.M. Gadi, also graduate students for their help in computer work.

I am thankful to Mr. Samak Omar and all the technicians of the Metallurgy workshop for their help in fabrication work. Glass blowing section deserves the whole credit for making the glass apparatus.

Service of Mr. F.M. Khalifa is acknowledged for the final stage of the work.

## Table of Contents

Chapter	-	1	Introduction	...	3
Chapter	-	2	Flask and outline of the work	...	1-1
Chapter	-	3	Synthetic and analytical Techniques	...	1-6
Chapter	-	4	Experimental	...	1-7
Chapter	-	5	Results	...	2-7
Chapter	-	6	Discussions	...	3-1
Chapter	-	7	Conclusions	...	4-4
			References	...	4-8

iii

# 1. INTRODUCTION

Since the development of two film mass transfer theory<sup>1</sup>, Chemical Engineers have undertaken many fundamental studies on mass transfer from a drop phase to a surrounding liquid phase under different hydrodynamic conditions, various models have been developed which may be extended to specific metallurgical systems also.

In any Blast furnace operation, Iron-ore is reduced to Iron and while coming down through the stack it picks up Si, Mn, S, P etc. from the burden. The molten iron in the form of droplets of different sizes passes through the hearth region and collects in the hearth. The slag that forms from the gangue materials collects at the top of the metal. In normal operation the quantity of slag is about 60-70% of the total iron tapped. So, it is expected that the metal is always covered with a thick layer of slag and all the droplets of Iron pass to cross the thick viscous layer before they <sup>are</sup> collected in the hearth.

The existence and formation of the droplets inside the blast furnace has been conclusively proved by many authors in the past. Schindler<sup>2</sup> while explaining the "Mechanism of the formation of iron shots in B.F and low shaft furnace slag" had given a good review of the previous work done in this field. Kosobrovitch<sup>3</sup> explained



The mechanism of desorption under B.F. <sup>Condition</sup> conditions on the basis of reaction and film theory and proved that mass transfer from droplets occurs in the stag phase.

1.1 The rate transfer between a single drop and the surrounding field will depend on the

- i) shape and the nature of the drop
- ii) Motion of the drop in the medium
- iii) Diffusional flux on the surface.

1.1a Shape and nature of the drop

There are many situations when the liquid droplets ~~are~~ passing through the continuous phase can not maintain its original shape. The shape will be ellipsoid and will oscillate along the major axis. Large drops can be considered to be oblate spheroid which may even <sup>oscillate</sup> ~~oscillate~~ to approximate prolate spheroidal form<sup>8</sup>. The oscillating drops show far greater rate of mass transfer than any other type. Galwey<sup>8</sup> observed that when the drop density is very high and the ratio of the drop viscosity to the aqueous phase viscosity is very small, then the drop may assume the prolate shape. The eccentricity ratio  $E^2$  as expressed by the author is

$$E^2 = \frac{\rho_2}{\rho_1} \left( 1 + \frac{\mu_2}{\mu_1} \right) = E^2 \left\{ \frac{1}{3} + \frac{2\mu_2}{5\mu_1} \left( \frac{\rho_2}{\rho_1} \right) + \frac{2}{5} \left( \frac{\mu_2}{\mu_1} \right)^2 + \frac{1}{15} \left( \frac{\rho_2}{\rho_1} \right)^3 \right\} \dots \textcircled{1}$$

When  $E^2$  is greater than 0, the distortion is prolate

and if  $E^2 < 0$ , the distortion is oblate.<sup>8</sup>

\* Take the list of nomenclatures given at the end of the text for explanation of the terms.

As the drop size increases, the eccentricity of the nonoscillating ellipsoidal drop increases. Garner and Gossamer<sup>5</sup> proposed the equation for calculating the area of such nonoscillating drops.

$$A = \frac{\pi}{2} \left[ a^2 b + \frac{a^2 b}{e^2 - 1} \ln \left( e + \sqrt{e^2 - 1} \right) \right] \quad (2)$$

The ratio of the area of an ellipsoid to that of a sphere of equal volume is

$$\frac{A}{A_0} = \frac{1}{2} \left[ e^{3/2} + \frac{1}{e^{3/2} - 1} \ln \left( e + \sqrt{e^2 - 1} \right) \right] \quad (3)$$

If the drop of low viscosity moves through a high viscous field a series of shape change is expected. The shape of the droplet affects the Sherwood number in a complex way, but the mass transfer co-efficient remains proportional to the (diffusivity)<sup>1/2</sup> and agrees well with the theoretical analysis of transfer across mobile interfaces<sup>6</sup>.

When the size of a drop falling in a low viscosity medium is increased beyond the laminar flow region, the drop begins to vibrate. The term vibration refers to periodic changes from oblate ellipsoid to prolate and back to original form along the axis of symmetry. Sanchez and Gossamer<sup>5</sup> developed the equation by using the primary mode of oscillation and expressed as:

$$\omega = k = \left[ \frac{72 \pi^2 \gamma}{(16\pi^2 + k^2) a^3} \right]^{1/2} \quad (4)$$

### 1.1.3. Motion of the drop

The motion of the liquid drop in the liquid medium has been studied extensively by Chemical Engineers as a part of liq-liq. extraction techniques. The motion of liquid mercury droplets in electrolytic solution is characterized by the existence of charge<sup>6</sup> on the liquid surface. The motion of liquid droplets<sup>7</sup> in the liquid medium is closely tied up with the size of the diffusional flux to the drop solution interface.

The effect of surface active material on the motion of drop had been studied by Levinsk and Goussakov.<sup>7</sup> It was observed that surface active materials may retard the motion on the surface of the drop when drop size is small. The surface active materials cannot retard the surface motion of a relatively large drop. Therefore, even in a medium containing such material, a large sized drop falls under the condition of unretarded surface motion. A model had been proposed by Tseng and Kintner<sup>8</sup> which accounted for the reduced mass transfer to drop falling in medium containing surface active agents. The reduction in the interfacial area and changes in velocity and circulation pattern were the causes of reduced mass-transfer. The theoretical and experimental values agreed with each other well within 10%.

For a spherical liquid drop moving in another liquid field, the boundary does not remain rigid. It moves from front to rear stagnation along the axis of symmetry creating continuously a new area. Rubenski and Hedemari had shown that a change in boundary condition on the surface of a drop leads to a significant change in the velocity of the falling drops. For the fall of a small liquid drop in a liquid medium under the gravitational force,  $T$ , the terminal settling velocity had been expressed as

$$T = \frac{2}{9} \frac{r^2 (\rho_D - \rho_L)}{\mu_L} \cdot \frac{\beta_L \beta_D \beta_D}{2(\beta_L + 3\beta_D)} \left( \frac{\rho_L}{\rho_D} \right) \left( \frac{\mu_D}{\mu_L} \right) \quad (8)$$

when the viscosity of the interior liquid is large,

$\beta_L \gg \beta_D$  the equation reduces to:

$$T = \frac{2}{9} g r^2 \left( \frac{\rho_D - \rho_L}{\mu_L} \right) \quad (9)$$

which is Stokes' law. The Stokes law correction factor for liquid drop had been calculated from analysis of Hedemari and Rubenski<sup>6</sup> and expressed as:

$$T_L = \left( \frac{\beta_L \beta_D + 3\beta_L}{3\beta_D + 2\beta_L} \right) T_S \quad (10)$$

For a low viscosity liquid drop falling in high viscosity liquid field, the correction factor of 1.3 had been determined for a fully circulating drop. If the viscosities of the two fields are equal the correction factor of 1.3 may be considered.<sup>8</sup> Very often, in spite

of low viscosity of the liquid drop, the Stokes law is applied because of the rigidity of the surface of the drop due to the presence of unavoidable impurities.<sup>9</sup>

Velocity pattern in drops falling through glycerine solution had been studied by Garner and Haycock<sup>10</sup> and their observations revealed that no circulation was possible until the fall velocity exceeded 0.5 cm/sec.

due to mobility of the interface, the velocity gradients present in the liquid are smaller than those in the case of solid interface. With the same driving force (gravity), the velocity of steady fall of a liquid drop should be greater than the velocity of fall of a solid sphere.<sup>9</sup>

the liquid on the surface of the drop moves at a velocity

$$\left( U_{\theta} \right)_{r=R} = U_0 \sin \theta \quad (8)$$

Where  $U_0$  is the magnitude of liquid velocity at the drop equator and  $U_{\theta}$  is the velocity on the surface of the drop at an angle  $\theta$  from the drop equator. Again,

$$U_0 = \frac{\Delta \rho}{2} \frac{g}{\mu_L + \mu_F} \quad (9)$$

Where  $\mu_L \gg \mu_F$ , the velocity on the surface is small and limit becomes zero in the case of solid surface.

### 1.1 C. Diffusional flux on the drop surface

Levich deduced the diffusional flux to the surface of a drop, falling in a liquid where  $R_0 \gg 1$ . The density of the liquid in the drop was considered to be higher than that of the liquid medium. The total flux  $I$ , on the surface of the drop was found to be :

$$I = 4 \pi (C_0 - C) \sqrt{\frac{D}{\pi}} \left( \frac{R_0 \gamma_0}{4} \right)^{1/2} v^{1/2} \quad (10)$$

If  $R_0 \gg 1$  and certain diffusion boundary layer exists on the surface of the droplet, its thickness  $\delta$  can be found out from the relation :

$$v_0 \frac{\delta}{r} \approx D \frac{C}{\delta^2} \quad (11)$$

For  $R_0 \gg 1$ , the velocity of the liquid  $v_0$  on the surface of the drop will be equal to the velocity of the falling drop. Hence by putting  $v_0 = v$  in equation (11) and by rearranging, the final form will be :

$$\delta = \sqrt{\frac{Dv}{v_0}} \quad (12)$$

The general equation for diffusional flux on the surface of the drop is  $I = \frac{4\pi}{\delta} (C_0 - C) R$  (13)

Substituting equation (12) in (13) and rearranging, the total flux on the drop surface in the case when  $R_0 \gg 1$  will be :

$$I = 4 \pi r^2 (C_0 - C) \left( \frac{Dv}{\delta} \right)^{1/2} \quad (14)$$



are in the state of internal motion. The continuous phase mass-transfer resistance follows closely that reported for solid sphere in the circulating regime where as the effective diffusivity within the drop is a constant multiple of the molecular diffusivity.<sup>12</sup>

It is possible in some cases that the mass-transfer resistance is in the drop phase. The overall transfer rate will be controlled by the extraction mechanism inside the drop and to a  $\frac{D_{AB}}{D_{AB}^0}$  extent by the hydrodynamics of the system. Both molecular and convective diffusivity may influence the transfer rate in the dispersed phase. Extraction efficiency can be expressed in terms of Weissenberg equation.<sup>13</sup>

$$E_d = 1 - \frac{C_1}{C_2} \sum_{n=1}^{\infty} \frac{1}{n^2} \exp \left( -4 \frac{v^2 n^2 D_p^2}{d^2} \right) \quad (14)$$

$E_d$  = fraction extracted (dimensionless).

The circulation model of Grossig and Grink<sup>14</sup> is valid when the relative motion of the drops induces circulation. Turbulence of high intensity in the continuous phase may cause turbulent movement inside the drop. Gaudin and Garon<sup>15</sup> proposed the model for mass-transfer under the above mentioned situation. The results from the series of experiment indicated that they do not agree with the above models. So an experimental factor  $\gamma$  has been introduced in the equation.  $\gamma$  when multiplied



with molecular diffusivity becomes more or less the effective diffusivity.<sup>15</sup>

Gurney and Govershof<sup>16</sup> studied the effect that droplet oscillation had on the continuous phase resistance. Ross and Richter<sup>14</sup> supported a model for vigorously oscillating single liquid drop, moving in a liquid field with the concept of interfacial stretch and internal droplet mixing. To predict the initial zero thickness for a spherical drop with uniform internal concentration of solute, two film theory was used. The liquid film thickness is predicted by using the empirical correlation of Gurney and Govershof which is:

$$V_{D0} = 0.6 \, x_{D0}^{\frac{1}{2}} \, x_{D0}^{\frac{1}{2}} \quad (15)$$

To predict the inside film thickness, the penetration theory is used with contact time equal to the time for one oscillation cycle. This contact time was chosen as a result of photographic study of the pattern of movement inside a falling oscillating drop. During each time, the droplet underwent a period of oscillation, the interior of the drop was violently mixed, so the interface will be renewed during each droplet oscillation. Hence,

$$x_D = .45 \, ( \, v_D \, W \, )^{\frac{1}{2}} \, \text{cm/sec.} \quad (16)$$

$W$  = frequency of oscillation in  $\text{rad/sec}$ .

Hence the over all mass transfer coefficient is

$$\frac{1}{K_0} = \frac{1}{K_0} + \frac{a}{K_0} \quad \text{where } a = \left( \frac{\partial A}{\partial A_0} - \frac{\partial A}{\partial A} \right) \frac{\text{drop phase}}{\text{slag phase}} \quad (27)$$

In Spas and Kintner model, one oscillation has been considered as surface life time and the area change resulting from one oscillation has been assumed constant. Angello and Lightfoot<sup>17</sup> modified the gas and Kintner concept and studied the penetration theory for surface stretch applied to oscillating droplets in the Reynolds number ranges between 200-2000. Further modification and studies in the Reynolds number range between 10-20 was conducted by ~~Spas~~<sup>18</sup> and Lightfoot<sup>19</sup> and they observed that the distortion of drop changes the Reynolds number by about 20%. All these studies have been made with liquids of low density and viscosity.

It has been known for quite sometime that the composition of the liquid metal at the hearth is very much different as compared to the metal at the hearth. Earlier workers tacitly assumed that the site for slag-metal reaction was the interface between the slag and the pool of metal. Therefore, they essentially simulated the slag and metal pool in the laboratory and studied the reaction kinetics. However, from mass transfer considerations, there was no reason<sup>20</sup> to ignore the chemical reaction while the metal droplets are passing through the slag. As a matter of fact, some recent studies<sup>(18)(20)</sup> have shown

that the desulfurization takes place primarily while droplets fall through the slag layer. When this work was undertaken no investigation in this direction could be located in the literature.

The situation is very complex involving thousands of droplets of different sizes and specific chemical and physical conditions. A clear understanding of the process may emerge through controlled drop studies. The knowledge gained from the performance of individual large drops may not be immediately applied to the complex operation. However, this is expected to be of considerable help to understand the mass-transfer situation. It is in this context, the decision was taken to examine the phenomena exhibited by single drop moving through the viscous liquid layer with the help of a solid model.

## 2.

### PLAN AND OUTLINE OF THE WORK

The difficulties of handling molten slag and metal at high temperature can be eliminated with the help of room temperature systems in which the densities and viscosities of the two phases should bear some resemblance to the actual process. Different techniques had been adopted to study the mass-transfer to or from the droplets and the bubbles. Constant volume experimental technique as adopted by Galanter<sup>(32)(31)</sup> and Coworker to study the mass-transfer from bubbles can be applied to droplets also. Scintillation technique for instantaneous measurement of exchange rate of the solute on freely suspended single drop has helped in studying the exchange process without affecting the hydrodynamics of the system<sup>(33)</sup>. Galanter<sup>(34)</sup> and Coworker observed that mercury drops formed one drop diameter above the continuous phase were not distorted while passing through the liquid surface.

In this study, mercury drops were formed above the surface of the aqueous phase in conformity with the actual blast furnace condition and the (i) Mass transfer from the droplets while passing through the aqueous phase (ii) Diffusion co-efficient of the solute in the aqueous phase (iii) Velocity and the residence time of the droplets in the aqueous phase were determined. The dropping rate was

is assumed that only one drop at a time passed through the aqueous phase.

### 2.1 Measurement of Mass Transfer Co-efficients.

In the experiments, mercury droplets were used to simulate the metal phase and water with its viscosity adjusted with glycerol was equivalent to the slag phase. Typical reactions which are conveniently used for studying mass transfer between slag and metal without production of gas at the interface are:



Where square brackets indicate the metal phase and round brackets the aqueous phase.

Schramm and Richardson<sup>(28)</sup> studied the mass transfer across interface agitated by bubbles in both systems represented by equations (18)-(19) under aqueous and metal controlled conditions.

For the process of mass transfer from the droplets, reaction (18) can be favourably used. In the studies of different droplet sizes were passed through aqueous phase of different periods ion and glycerol concentrations. In the series of experiments it was planned to verify whether aqueous control condition existed in the system

or not.

The small amalgam pool formed at the bottom of the apparatus was kept separated from aqueous solution in order to avoid any reaction between the two liquids.

### 2.2 Diffusion Coefficient of $Fe^{3+}$ ion.

During the course of experiment, the concentration of ferric ion in the aqueous phase is supposed to be reduced, hence the diffusion coefficient of ferric ion is expected to vary. So, it is essential to determine the diffusion co-efficient of ferric ion as a function of concentrations in the aqueous phase. Diffusion co-efficient of ferric ion of various concentrations under different glycerol content similar to experimental conditions for mass transfer study were carried out by photographic technique.

### 2.2 Velocity and residence time.

Knowledge of velocity and residence time for the droplets in the aqueous phase is important in order to determine the hydrodynamics and the mass transfer results. Photographic techniques were adopted for the measurements of terminal velocity and the residence time of the droplets in the aqueous phase.

### 3. REAGENTS

The aqueous solutions used for studying the reaction in equation (10) consisted of  $\text{FeCl}_3$  at various concentrations ranging from 10-70 m-moles/liter and A.R. grade glycerol between 25-75 wt percent for adjusting the viscosities of the aqueous phase. The pH of all the solutions were adjusted to 1.4 by adding A.R. grade HCl before every experiment. All aqueous solutions were deaerated prior to use by passing purified nitrogen for 2 hours.

The amalgams were prepared from triple distilled mercury and iodine of 99.999 percent purity.

#### 3.1 Analytical techniques.

Polarographic techniques were used for measuring the concentrations of  $\text{I}^{+}$  and the diffusion co-efficients of ferric ions in the aqueous phase. The apparatus consists of a mercury reservoir fitted with a capillary tube at the bottom and a calomel electrode in one branch of U tube and the other branch is the sample container separated by porous disc. Mercury drops are the dropping electrode formed from the capillary of 0.05-0.06 mm bore under constant pressure and time interval. Calomel electrode has been provided to eliminate the possibility of unknown or nonreproducible anode potential, hence it acts as reference electrode. In polarography actually

the current vs. E.M.F plot is recorded (26)

A concentration gradient is established between the dropping electrode surface and the bulk solution. At equilibrium, the rate of discharge of ions by current is equal to the rate of diffusion to the electrode surface. For relatively small values of current, the concentration overpotential is small and as the applied E.M.F is increased beyond the decomposition potential, the current exhibiting the normal  $\text{Rise}_{\text{and}}$  stage is reached at which the concentration overpotential increases rapidly and the current reaches a limiting value, hence this is the maximum rate at which particular ion can be discharged under the given experimental conditions. As the concentration of the bulk solution increases, the limiting current also increases. The galvanometer is unable to follow the periodic growth and fall of the current of each individual drop, so the saw toothed waves are observed. This in measuring the diffusion current, the average of the galvanometer oscillation is to be considered (27).

In order to obtain true diffusion current of a substance, a correction must be made for the residual current. The most reliable method for making this correction is to evaluate in a separate polarogram the residual current of the supporting electrolyte alone. The value of the residual current at the particular half wave potential



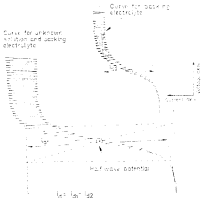


FIG. 1 CORRECTION TECHNIQUE FOR THE DETERMINATION OF CONCENTRATION AND DIFFUSION COEFFICIENT FROM POLAROGRAM

level of the corresponding element is subtracted from the total observed current<sup>(197)</sup>. Fig. 1 indicates the correction techniques for the determination of diffusion current. Correction technique has been adopted for the determination of concentration and diffusion coefficients.

All the electroactive materials have their half wave potential. This is the potential at the point of current-voltage curve, half the distance between the residual current and the final limiting current. Hence it is customary to measure diffusion current at the half wave potential level. In the case of Pb, the value of half wave potential changes with pH. At pH 3.5-4, half wave potential is +.43 volts<sup>(198)</sup> and +0.36 volts for Ferric ion at pH=4<sup>(199)</sup>. For the determination of concentration of Pb in the aqueous phase, the pH of the solution has to be maintained at 4.4 and with backing electrolyte, the resultant pH was within 3.5-4.

Before each experiment, the solution is deaerated by passing purified nitrogen for 15-20 minutes.

#### 4. Description of the apparatus.

The apparatus used for manometric study is shown in Fig. 2. It is a 15 cm long tube of 4 cm diameter resting on a container for storing the used amalgam. Suitable siphoning arrangement has been provided to drain out the amalgam from the column at proper interval.

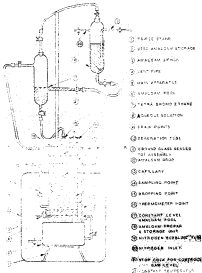


FIG. 2. SCHEMATIC DIAGRAM OF THE APPARATUS.

Since the Hg-In amalgam gets oxidized very easily in air, suitable arrangement has been made to maintain nitrogen atmosphere on the liquid column. Since the desorption of the solution is required before each experiment, suitable provision has been made for this purpose. There are three openings at the top of the apparatus. The centre hole for dropping amalgam and the other two are for sampling and thermometer point. The whole apparatus is completely air tight and immersed in constant temperature bath.

The auxiliary part of the apparatus is the amalgam preparation and dropping unit. The amalgam is stored on separate column and drops into the dropping column after certain interval of time in order to maintain more or less constant level in it. The height of the amalgam column from the top level of the amalgam pool to the tip of the capillary was maintained at 30 cm. Provisions are there to maintain nitrogen atmosphere on the amalgam storage and in the dropping unit.

The whole apparatus is made up by Pyrex glass and suitable ground glass joints has been used for assembling purposes.

#### 4.1 MANIPULATION TECHNIQUE

Before starting the experiment, a layer of "Tetra-~~base~~-ether" of 2 mm thickness was made at the bottom of the apparatus in order to separate the amalgam

pool from the aqueous solution. Tetra bromo ethane is of density 3.8, reacts neither with aqueous phase nor with the amalgam. Hence, the mass transfer only from the droplets can be studied.

In all the experiments 200 cc of aqueous solution containing different proportions of glycerol and  $\text{FeCl}_3$ , after adjusting the pH to 1.4 was poured slowly on the top of the tetra bromo ethane. The height of the aqueous column was 50 cm in all the cases. The solution was thoroughly deaerated by passing purified nitrogen for two hours.

Some experiments were conducted at 21-22°C in the present apparatus, where appreciable amount of transfer could not be detected. With a column height of 50 cm, sufficient amount of transfer was recorded with 50 cc aqueous solution at a temperature of 31-32°C. Since it was difficult to fulfill the experimental requirements in the tall column, experiments at higher temperatures were tried. Hence all the experiments were conducted at 36°C. It was possible to control the temperature of the constant temperature bath upto  $\pm 0.1^\circ\text{C}$ .

Capillaries of 1 mm and 0.8 mm inside diameter were used for dropping amalgam. All the capillary tips were polished and cleaned. Satisfactory results were

Amalgam was prepared by pouring the weighed amount of mercury on the ladle under nitrogen atmosphere, blowing by purified nitrogen into the stored amalgam for 1-2 minutes was preferred to ensure thorough mixing. No corrosion formation on the surface of amalgam storage was detected. Storage column and the dropping unit remained under nitrogen atmosphere through out the experiment.

As soon as the preparation of amalgam was over, certain amount of amalgam was drawn out from storage to the dropping unit, deaerated the capillary and the connecting rubber hose. This amalgam was stored separately and subtracted from the total amount in order to calculate the actual amount of amalgam used in each experiment. Before starting the experiments, 5-10 drops of amalgam were collected in the weighing bottles under identical condition in order to determine the equivalent diameter of the droplets. Identical dropping rate could not be maintained in all the experiments but in individual experiments same drop rate from the beginning to the end was maintained. Drop rate varied between 100-150 per minute in the case of small capillary and 100-150 per minute for the bigger one. The above mentioned dropping rate was sufficient to ensure the passage of a single droplet through the liquid column at a time. The amount of amalgam passed through the solution varied between 1040-1570 gms in the case of small

capillary and 1800 - 2000 ga for the big one. The experiments with small capillary continued from 270-300 minutes and with big capillary from 80 - 110 minutes.

Subramaniam and Richardson<sup>(28)</sup> work indicated that the initial concentration of In in the amalgam had no effect on the observed rates of hydrogenation. Two experiments were tried with different In concentrations and the same results were obtained. Hence it was decided to conduct all the experiments with In concentration of 0.001.

Viscosity of the liquid phase ~~was varied~~ from 0.75 cp to 11.75 cp and ferric ion concentration from 10-70 m. moles per liter.

In all the experiments, after passing amalgam through the aqueous solution for certain interval of time, 1 cc of the solution was drawn out through the sampling hole and analysed polarographically for indium content. The characteristic half wave potential of  $\text{In}^{3+}$  and  $\text{Fe}^{2+}$  are widely separated. To prevent  $\text{Fe}^{2+}$  from oxidizing the dropping mercury electrode, 2M potassium chloride containing 50 ga/liter of hydroxy acetic acid was used as a backing electrolyte<sup>(28)</sup>. The addition reduced the ferric ion to  $\text{Fe}^{2+}$ . The diffusion current varied linearly with concentration and was not affected by glycerol content. Correction method as indicated earlier was followed to determine the  $\frac{i_{\infty}}{C}$ ; diffusion current for indium ion. Again

polarographically determined the diffusion current for ferric ion of a standard indium chloride solution of known concentration in the presence of a backing electrolyte of 1 M HCl/liter. Similarly correction factor was adopted in finding out the net diffusion current. Then from the relation

$$\frac{C_1}{C_2} = \frac{Id_1}{Id_2}$$

where  $C_1$  = Concentration of ferric ion in unknown solution in m. moles/liter. (~~with-moles/liter~~)

$C_2$  = Concentration of ferric ion in standard solution of known concentration, in m.moles/liter.

$Id_1$  = diffusion current for unknown solution in microampere.

$Id_2$  = Diffusion current for known solution in micro amp.

the concentration of ferric ion in the aqueous phase was determined. This procedure was adopted in all the samples. By stoichiometry, from the concentration of ferric ion, the amount of ferric ion consumed after certain interval of time was calculated.

#### 4.2 Diffusion coefficient of ferric ion.

In the mass transfer experiments it was observed that the concentration of ferric ion in the aqueous phase was decreasing, hence the diffusion co-efficient values might also change.  $D_{Fe^{3+}}$  values are available only at 30°C. Since all the mass transfer experiments were carried out



at 35°C, so the  $I_{D_{Fe}^{3+}}$  values at different concentrations of ferric ion and glycerol were determined by polarographic technique at 35°C.

In the series of experiments, concentrations of ferric ion were varied between 0.05- 01.5 m. moles/liter in water, 12.5 + 01.5 in water + 50% wt glycerol and 12.5 + 04 m. moles per liter in water + 70 wt per cent glycerol medium. The supporting electrolyte (2M) was 0.05M per liter sodium oxalate and .005% gelatine as matrix supportant. It was observed that .005% gelatine was sufficient for water and water + 50 wt % glycerol medium but in case of 70 wt % solution, the gelatine addition was increased to .01 % . The pH of the solution was adjusted to 4 by adding acetic acid before each experiment.

Known volume of solution was taken in the sample holder and deaerated for 15 minutes before the start of the experiment. Temperature control was 35°C  $\pm$  .5°C. The drop time and weight of mercury passed per second were determined. Correction method was adopted in determining the  $mi^2$  diffusion current for each sample from the Polarograms. From the law governing the condition of diffusion at a dropping mercury electrode and periodic growth and fall of the droplets, theoretical equation for diffusion current as developed by Ilkovic (27) is:

$$I_d = 607 F D_{Fe}^{3+} C m^{2/3} t^{1/6} \quad (22)$$

$i_d$  = diffusion current in micro amperes during the life of the drop,

$F$  = number of Faraday electricity required per mole of the electrode reaction,

$C$  = concentration in millimoles per liter,

$m$  = rate of flow of mercury in m.g/sec.,

$t$  = drop time in sec.,

$D_{Fe^{3+}}$  = diffusion co-efficient of ferric ion in  $\text{cm}^2/\text{sec.}$

From eqn. (25),

$$D_{Fe^{3+}}^{\frac{1}{2}} = \frac{I_d}{4\pi^2 F \cdot C \cdot m^{1/2} t^{1/2}} \quad (26)$$

$D_{Fe^{3+}}$  for all the solution are calculated and reported in table no.3. The plot  $D_{Fe^{3+}}$  vs concentration is shown in fig. 4 which helped in determining diffusion co-efficient at any concentration within the experimental range. The reproducibility of diffusion current values were checked and these were within  $\pm 1\%$ .

#### 4.5 Velocity and Residence Time Determination-

The terminal velocity and the residence time of the droplets of different sizes in the different aqueous media, similar to mass-transfer experimental conditions were determined by photographic means. Several photographic exposures at regular time intervals of a drop falling through the aqueous phase were taken by using SINOGRAPH- Type 1501-4B (General Radio Company) in a darkened room. For

bigger drops 8000 <sup>Caricofolium</sup> ~~frames~~ and for the smaller ones 4000 <sup>Microscopium</sup> ~~frames~~.  
Settings were used. The photographs are shown in  
Fig. 5a,b. The photographic studies revealed that the  
small drops were reaching their terminal velocities within  
in 1-1.5 cm travel distance from the liquid surface, the  
corresponding travel distance was 3-3.5 cm in the case of  
big drops. Residence time and the terminal velocities  
were calculated from drop intervals and the microscope  
C<sub>mag</sub>  
values for all the cases and reported in Table 1.b

Movie Camera was used in determining the  
change of shapes of the droplets when were taking place  
during its passage through the aqueous phase by using  
Microscope. It was possible to observe the changes in  
shape at different positions of the liquid column but  
due to certain limitations, complete shape changes could  
not be recorded hence shapes could not be measured.

\* Some interesting movie photographs are shown in Fig. 4.



# SLIP SLID COMPLETE



Fig. 2a,b- terminal velocity and resistance time determination by photographic techniques.



Fig. 4 shows the ventilation and changes in shape also during its passage through the aqueous phase (water + NaCl).

Properties of the 400000 glass\* and other  
Experimental data are given in table 1a and 1b.

Table 1a

Run No.	Percent glycerol	Weight of glycerol lost in 10.000 g per liter	Viscosity in 1.0 in 1.0	Density in g/cm <sup>3</sup>
1	70	80	14.75	1.175
2	70	75	11.75	1.13
3	70	10	11.75	1.13
4	70	25	11.75	1.175
5	water	25	.750	1
6	25	25	2.00	1.00
7	50	25	2.00	1.00
8	water	25	.750	1
9	water	25	.750	1

\* Viscosity and density data taken from handbook of  
Chemistry and Physics, Forty third edition.

TABLE 22

Log No.	Group 121 50-50	Group 122 50-50	Group 123 50-50	Group 124 50-50	Group 125 50-50
1	.159	122	1222.1	47.42	.159
2	.160	123	1270	47.42	.159
3	.159	124	1100.5	47.42	.159
4	.158	125	1220.7	47.42	.159
5	.157	126	1204	70.2	.157
6	.159	127	1179	51.2	.159
7	.200	128	2000.2	72.47	.160
8	.201	129	1804.8	72.47	.157
9	.158	130	1042	70.2	.157



results from mass transfer experiments are shown  
in table II

TABLE II

EXP.NO.	CONC. OF $Fe^{3+}$ in aqueous phase in m. moles per liter	INITIAL SOURCE IN CONC. IN moles per liter ( $Fe^{3+}$ ) <sub>0</sub>	$\frac{(Fe^{3+})_0}{(Fe^{3+})_{\infty}}$ to	TIME IN sec.
1	.14	25	0.4823	3000
	.276	25	0.9099	6000
	.34	25	0.9880	9000
	.824	25	0.9015	15000
	.89	25	0.9923	17000
2	1.5076	75	0.9508	1700
	1.4168	75	0.9421	10400
	1.829	75	0.9507	10700
	2.2797	75	0.9421	17000
	2.1021	75	0.9508	17000
3	1.829	10	0.9999	15000
	1.829	10	0.9999	15000
	1.829	10	0.9999	15000
	1.829	10	0.9999	15000
	1.829	10	0.9999	15000
4	1.829	25	0.9508	17000
	1.829	25	0.9508	17000
	1.829	25	0.9508	17000
	1.829	25	0.9508	17000
	1.829	25	0.9508	17000
5	1.829	25	0.9508	17000
	1.829	25	0.9508	17000
	1.829	25	0.9508	17000
	1.829	25	0.9508	17000
	1.829	25	0.9508	17000
6	1.829	25	0.9508	17000
	1.829	25	0.9508	17000
	1.829	25	0.9508	17000
	1.829	25	0.9508	17000
	1.829	25	0.9508	17000
7	1.829	25	0.9508	17000
	1.829	25	0.9508	17000
	1.829	25	0.9508	17000
	1.829	25	0.9508	17000
	1.829	25	0.9508	17000
8	1.829	25	0.9508	17000
	1.829	25	0.9508	17000
	1.829	25	0.9508	17000
	1.829	25	0.9508	17000
	1.829	25	0.9508	17000
9	1.829	25	0.9508	17000
	1.829	25	0.9508	17000
	1.829	25	0.9508	17000
	1.829	25	0.9508	17000
	1.829	25	0.9508	17000

Plots  $\log \frac{(Fe^{3+})_0}{(Fe^{3+})_{\infty}}$  vs. time are shown in fig. 2a, 2b

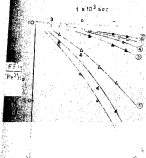


FIG. 5a. RESULTS OBTAINED FROM REACTION 18. SMALL DEPLETES OF Fe<sup>3+</sup> AND Fe<sup>2+</sup> IN MANGANESE DEFICIENT PHASE .75-0.75. PLOTTED IN 10<sup>3</sup> log OF THE RATIO. INDICATE THAT THE RATIO OF Fe<sup>3+</sup> TO Fe<sup>2+</sup> IN THE MANGANESE DEFICIENT PHASE IS APPROXIMATELY 0.5.

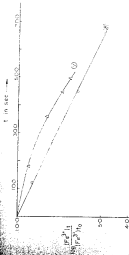


FIG. 3b. RESULTS OBTAINED FROM REACTION (4) FOR DIS. NO. 10, WITH 0.2 M/L IN AMALGAM. ADDITIONAL DATA FROM 2.0 M/L IN DIS. NO. 10, IN TERMS OF EQUATION (24), YARNER'S NUMBER, THE DATA FROM EXPERIMENT NUMBER 10, DESCRIBED FOR EQUATION (4).

Polarographic results for the diffusion co-efficients of ferric ion in the different aqueous media are in table No. III a,b,c.

TABLE III a

In water at 30°C  $\pm .5^\circ$

S-1- No.	Conc. of Fe <sup>3+</sup> in 500% vol% per liter,	Diffusion co-efficient in cm <sup>2</sup> /sec.
1	6.25	$7.0689 \times 10^{-6}$
2	12.50	$6.9433 \times 10^{-6}$
3	18.75	$6.8092 \times 10^{-6}$
4	25.00	$6.5474 \times 10^{-6}$
5	31.25	$6.2992 \times 10^{-6}$

TABLE III b

In 25 wt% glycerol + water at 30°C  $\pm .5$

1	12.5	
2	18.75	$2.768 \times 10^{-6}$
3	25.00	$2.6171 \times 10^{-6}$
4	31.25	$1.8600 \times 10^{-6}$

TABLE III c

In 75 wt percent glycerol at 30°C  $\pm .5$

1	12.5	$6.8148 \times 10^{-7}$
2	18.75	$5.4300 \times 10^{-7}$
3	25.00	$7.8038 \times 10^{-7}$
4	31.25	$4.3640 \times 10^{-7}$
5	37.50	$1.7013 \times 10^{-7}$

Values of Diffusion co-efficient vs concentrations of ferric ion from table III a,b,c have been plotted and shown in Fig. 4

$D_{H_2O}$  ( $10^6$  cm<sup>2</sup>/sec.)

70 wt % H<sub>2</sub>SO<sub>4</sub>

25 wt % H<sub>2</sub>SO<sub>4</sub>

Water

FIG. 4. DIFFUSIVITY OF SULFURIC AC. AT 35°C. IN 25, 70, AND 100% SULFURIC AC. AND WATER.

## 6. Discussion of the results

### A. Kinetic steps.

The reaction being studied is



the kinetic steps are

- 1) transport of  $\text{Fe}^{3+}$  ions to the interface from the aqueous phase (bulk)
- 2) transport of  $\text{H}^+$  from the bulk aqueous to the interface
- 3) reaction at the interface (eqn.18).
- 4) transport of  $\text{Fe}^{2+}$  from the interface to the aqueous phase
- 5) transport of  $\text{In}^{3+}$  from the interface to the aqueous phase.

The chemical reaction at the interface (step 3) is expected to be very fast because it essentially involves electron exchange amongst atoms and simple ions. Abramowitz and Richardson<sup>(22)</sup> also found it to be very fast. Hence step(3) is not at all expected to be rate controlling.

If the process is solely transport controlled, then chemical equilibrium amongst the various species may be assumed. The equilibrium relationship for the reaction in equation (18) is as follows;

$$K = \frac{(\text{In}^{3+})_1 (\text{Fe}^{2+})_1^2}{(\text{In})_1 (\text{Fe}^{3+})_1^2} = \text{In}^{3+} \quad (19)$$

Where  $K$  is the equilibrium constant for the reaction (19). The brackets indicate the concentration of the species in the aqueous and metal phases and the suffix  $i$  indicates the concentration of the species at the interface in gram mole per c.c.

Because  $\text{In}^{3+}$  and  $\text{Fe}^{2+}$  are moving out from the interface to aqueous phase,  $(\text{In}^{3+})_i$  and  $(\text{Fe}^{2+})_i$  must be greater than  $(\text{In}^{3+})_{\text{bulk}}$  and  $(\text{Fe}^{2+})_{\text{bulk}}$  respectively and hence must be greater than zero as soon as the experiment has commenced. Since  $K$  is very large, and the numerator in eqn. (20) cannot be infinity, therefore the denominator must be tending to zero. This is possible provided either  $[\text{In}]_i^{2+}$  or  $[\text{Fe}^{2+}]_i$  tend to zero.

If the rate of transport of  $\text{Fe}^{2+}$  is less than that of  $\text{In}$  in the amalgam, then  $(\text{Fe}^{2+})_i$  would tend to zero and  $[\text{In}]_i$  would be close to  $[\text{In}]_{\text{bulk}}$ . For rate calculations, we may take  $(\text{Fe}^{2+})_i = 0$  without any significant error. The question is under such circumstances which transport step is rate-controlling? Step (3) has already been assumed too fast. As regards, transport of  $\text{Fe}^{2+}$  and  $\text{In}^{3+}$  [Steps (4) and (5)] are concerned, it may be stated that they are able to adjust themselves to match the rate of transport of  $\text{Fe}^{2+}$ . The adjustment would be achieved because the values of  $(\text{Fe}^{2+})_i$  and  $(\text{In}^{3+})_i$  can go up to their respective limits of solubility. Even if the solubility limits are reached, removal of  $\text{Fe}^{2+}$  and  $\text{In}^{3+}$  from the interface is possible by precipitation from solution. In this investigation, no precipitation effect was found. Hence the values of  $(\text{Fe}^{2+})_i$  and  $(\text{In}^{3+})_i$  were below their respective solubility limits. Hence

It can be concluded that step (4) and (5) would adjust themselves to match the rate of step (1) and hence step (1) would be the rate-controlling step with  $(\text{Fe}^{3+})_i \rightarrow 0$ . This has been called "aqueous control" by Suckerman and Richardson<sup>22</sup>.

A reverse situation can also be conceived where the rate of transport of I<sub>2</sub> in the amalgam is much slower compared to that of  $\text{Fe}^{3+}$ . Following the arguments given above, it can be similarly shown that transport of I<sub>2</sub> in the amalgam would be rate-controlling with  $[\text{I}_2]_i \rightarrow 0$ . This has been termed as "metal control" by Suckerman and Richardson<sup>22</sup>.

A third possibility is mixed-control of step (4) and (5) where the values of both  $[\text{I}_2]_i$  and  $(\text{Fe}^{3+})_i$  tend to zero.

In this investigation, the aim has been to study the aqueous control only and in order to achieve this the concentration of iodine in the amalgam was kept high.

## B. Evaluation of mass-transfer coefficient from experimental data.

Mass-transfer coefficients have been calculated from the change of concentration of iodine in the aqueous phase. This section presents the various equations that correlated experimental variables with mass-transfer coefficients.

Case I : Transport of  $\text{Fe}^{3+}$  in aqueous solution rate-controlling

If the number of droplets per unit time be  $n$  per sec. and the residence time of one droplet in aqueous column be  $T$  sec, then the number of droplets in the bath at any moment would be equal to  $nT$ .



$$= 3.4 \times 10^{-4}$$

Since the transport of  $\text{Fe}^{2+}$  is rate controlling and  $(\text{Fe}^{2+})_i \approx 0$ , hence

$$[\text{Fe}^{2+}] = k_{\text{Fe}}^{2+} [\text{Fe}^{3+}] \quad (33)$$

where by total solubility of  $(\text{Fe}^{2+})$  in the aqueous solution

$$\pi r^2 d^2 k_{\text{Fe}}^{2+} \frac{d[\text{Fe}^{2+}]}{dt} = - V_a \frac{d[\text{Fe}^{3+}]}{dt} \quad (34)$$

where  $[\text{Fe}^{3+}]$  = mass  $\text{cm}^{-3}$  of ferric ion

$d$  = diameter of the droplets in cm,

$k_{\text{Fe}}^{2+}$  = mass transfer co-efficient for ferric ion in cm,  $\text{sec}^{-1}$ ,

$[\text{Fe}^{3+}]$  = concentration of ferric ion in the aqueous phase

whose transfer was rate controlling in a, before/after

$t$  = time in sec,

$V_a$  = volume of the aqueous phase in c.c.

By rearrangement and integrating within the limits it could be expressed as

$$\log \frac{(\text{Fe}^{2+})_t}{(\text{Fe}^{2+})_{t_0}} = - K' t, \quad (35)$$

where subscript  $t_0$  and  $t$  denote the concentration at initial and

final times and  $K' = \frac{\pi r^2 d^2 k_{\text{Fe}}^{2+}}{4.535 V_a}$

From the plots in Figure 3a, 3b,  $K'$  being the slope and  $k_{\text{Fe}}^{2+}$  can be calculated from the experimental values of  $n, d, r, a$  etc as mentioned in the experimental chapter. The concentration of  $\text{Fe}^{2+}$  in the aqueous phase at different interval of time were determined polarographically and the concentrations of ferric ion were calculated from stoichiometry as in eqn (33) (for details refer to chapter 4.)

Integration of denaturation ratio of Dore's law can be plotted against the weight of analges passed per unit time instead of the case as shown in Fig. 8a, 8b. The total weight of analges passed during the course of the experiment over the period of 4 sec will be

$$W = \int_0^4 Q^2 dt \times 10.6 = W \quad (26)$$

Where W is the weight of analges in gm.

From eqn. (25)

$$-X^2t = - \frac{.0047 \times 10^{-2} K_{20} Z^2}{2.303 V_A} t \quad (27)$$

Substituting eqn. (26) in (27) and rearranging

$$-X^2t = - \frac{.0047 \times 10^{-2} K_{20} Z^2}{2.303 V_A} W \quad (28)$$

Hence eqn. (28) is modified and expressed as

$$\log \frac{(Fe^{2+})_{final}}{(Fe^{2+})_{initial}} = - \frac{.0047 \times 10^{-2} K_{20} Z^2}{2.303 V_A} W \quad (29)$$

Plot  $\log \frac{(Fe^{2+})_{final}}{(Fe^{2+})_{initial}}$  vs W should be straight line and from the slope  $K_{20} Z^2$  could be calculated when the other terms like  $d_0$ ,  $T$ ,  $V_A$  etc. were experimentally determined.

Case 3: Transport of  $Fe$  in the analges rate controlled.

The mass transfer co-efficient for Indian  $[Fe]$  could be calculated similarly by mass balance as before. The concentration of Indian in the drop phase would be constant in each experiment, since the transport of Indian is rate controlling and  $[Fe]_i \propto 0$  hence

$$J_{In} = K [In]_l^2 - [In]_d^2 \quad (10)$$

the iodine balance equation expressed as

$$V d^2 [In]_d / dt^2 + K [In]_d^2 dt = - V_m d [In]_d / dt \quad (11)$$

where  $K [In]_d^2$  = mass transfer co-efficient for iodine in drop phase.

$[In]_d$  = conc. of In in the amalgam facing the droplets  
in weight percent,

$V_m$  = volume of the drop in c.c.

$t$  = time in sec.

$d$  = diameter of the drop in cm.

By rearrangements and integrating within the limits

$$\log \frac{[In]_t}{[In]_{t_0}} = -K^* t \quad (12)$$

where the subscripts  $t_0$ ,  $t$  denotes the concentrations in

initial and final time and  $K^* = \frac{V d^2 K [In]_d}{2.326 V_m}$

from the plot  $\log \frac{[In]_t}{[In]_{t_0}}$  vs  $t$ , the slope is  $K^*$ , hence  $K \frac{d^2}{V_m}$  can be calculated.

Concentration of iodine after an interval of time can be obtained either by analyzing the used amalgam or by analyzing its concentration in the aqueous phase by polarography.

### C. Nature of non-linear data

The results with reaction in eqn. (10) with 0.08% iodine in amalgam and ferric ion varying between 10-75m. moles per liter in the aqueous phase (1.75-11.75 cps) are plotted in fig. 2a, 2b where  $\log \frac{[Fe^{2+}]_t}{[Fe^{2+}]_{t_0}}$  are shown as function of time.

## TABLE 4

The difference values calculated from Fig. 3a,  
 by using

Exp. (1) No.	$(\rho_{\text{exp}})_{\text{in m. sec.}}^2$ per liter for exp. points	$(\rho_{\text{exp}})_{\text{in cm}^2/\text{sec.}}^2$	$(\rho_{\text{exp}})_{\text{in cm}^2/\text{sec.}}^2$	$(\rho_{\text{exp}})_{\text{in cm}^2/\text{sec.}}^2$	$(\rho_{\text{exp}})_{\text{in cm}^2/\text{sec.}}^2$
					$\frac{\rho_{\text{exp}}^2 - \rho_{\text{exp}}^2}{\rho_{\text{exp}}^2 + \rho_{\text{exp}}^2}$
<b>exp. 1955</b>					
1	24.0425	$4.74 \times 10^{-7}$	$1.36 \times 10^{-2}$	17.30	15.877
	24.245	$4.80 \times 10^{-7}$	$1.36 \times 10^{-2}$	21.80	
	23.8075	$4.64 \times 10^{-7}$	$1.49 \times 10^{-2}$	21.90	
	22.610	$4.69 \times 10^{-7}$	$1.55 \times 10^{-2}$	22.50	
	22.325	$4.60 \times 10^{-7}$	$1.55 \times 10^{-2}$	27.40	
2	-	$1.52 \times 10^{-7}$	$1.04 \times 10^{-2}$	26.4	26.4
3	6.550	$7.48 \times 10^{-7}$	$2.13 \times 10^{-2}$	24.7	23.61
	6.495	$7.60 \times 10^{-7}$	$2.03 \times 10^{-2}$	24.9	
	6.420	$7.55 \times 10^{-7}$	$2.04 \times 10^{-2}$	44.0	
	6.505	$7.67 \times 10^{-7}$	$4.87 \times 10^{-2}$	45.1	
4	26.475	$4.77 \times 10^{-7}$	$1.50 \times 10^{-2}$	17.15	27.86
	26.65	$4.80 \times 10^{-7}$	$1.70 \times 10^{-2}$	24.80	
	26.6425	$4.80 \times 10^{-7}$	$2.34 \times 10^{-2}$	21.60	
	21.6625	$4.12 \times 10^{-7}$	$2.85 \times 10^{-2}$	27.20	
5	20.8775	$4.65 \times 10^{-7}$	$1.24 \times 10^{-1}$	29.20	21.69
	16.80	$4.60 \times 10^{-7}$	$1.60 \times 10^{-1}$	29.20	
	16.955	$4.60 \times 10^{-7}$	$1.70 \times 10^{-1}$	24.80	
	10.07	$7.90 \times 10^{-7}$	$1.80 \times 10^{-1}$	72.40	
6	22.5625	$2.45 \times 10^{-6}$	$4.45 \times 10^{-2}$	41.70	22.27
	22.7375	$2.45 \times 10^{-6}$	$5.15 \times 10^{-2}$	49.60	
	17.2175	$2.62 \times 10^{-6}$	$4.45 \times 10^{-2}$	24.50	
	14.8975	$2.12 \times 10^{-6}$	$12.80 \times 10^{-2}$	62.20	
7	22.925	$2.42 \times 10^{-6}$	$4.27 \times 10^{-2}$	42.45	23.16
	22.43	$2.68 \times 10^{-6}$	$12.15 \times 10^{-2}$	62.75	
	17.8925	$2.65 \times 10^{-6}$	$12.15 \times 10^{-2}$	71.65	
	16.8975	$2.64 \times 10^{-6}$	$12.10 \times 10^{-2}$	77.10	
8	-	$4.46 \times 10^{-6}$	$1.82 \times 10^{-1}$	52.12	52.12
9	22.9725	$4.00 \times 10^{-6}$	$1.25 \times 10^{-1}$	21.015	20.12
	-	-	-	-	
	14.2625	$4.62 \times 10^{-6}$	$1.69 \times 10^{-1}$	62.53	
	11.8475	$4.64 \times 10^{-6}$	$1.75 \times 10^{-1}$	63.453	

The derived mass-transfer coefficients are given in table 4.

If the specific surface available,  $S_{sp}$ , a change in the concentration of iodine in amalgam should not affect the rate of mass-transfer. In order to verify this, the concentration of iodine was increased by a factor of 5 in two experiments. In one case the best estimated slightly negative  $K_{sp}$  values for expt. no. 5 and 6) and can be ignored. In the other case (Compare  $K_{sp}$  values of expt. 10a and 4b, the rate increased by approximately 30 percent. However it may be partly due to some decrease in drop size in expt. 10a. Therefore, it can be safely concluded that the influence on rate because of a change in  $C_{I_2}$  is not significant. The little variation may be due to some other surface effect because of higher concentration of iodine in the amalgam.

$$\text{Further more, according to eqn.(25), } \log \frac{(Fe^{2+})_t}{(Fe^{2+})_{\infty}}$$

should vary linearly with  $t$  and should be independent of initial  $(Fe^{2+})$  concentration provided other factors such as drop size, viscosity etc. are kept constant. At 70 wt percent glycerol and small drop size, several experiments were conducted at ferric ion concentrations of 10, 25 and 75 g. ml.<sup>-1</sup>. The table 30a shows the mass transfer co-efficient decreases systematically with increase in concentrations. However, it has to be recognized that part of this variation is a result of decrease of diffusion co-efficient with increase in concentration. Fig.4 shows the variation of diffusion co-efficient of ferric ion with change in concentration in different aqueous media.

If all other factors remain constant, then  $K_{ps}Z\sqrt{D^2_{ps}Z}$  should be constant<sup>4</sup>. Table 4 compares  $K_{ps}Z\sqrt{D^2_{ps}Z}$  and it can be seen that  $K_{ps}Z\sqrt{D^2_{ps}Z}$  does not too vary much and vary systematically for exp. 1-4. Therefore, from this point of view, the experiments 1-4 do not seriously violate the aqueous control condition.

Figures 2a, 3a show that the curves mostly show some systematic deviation from linearity. Computer programming with various orders indicated that second order polynomial gives best fitting with the experimental results. The slopes and the mass transfer coefficients at various intervals were calculated by computer and given in table 4. The table shows that  $K_{ps}Z$  increases with time except for experiment 2a,3 and 5 where  $K_{ps}Z$  remains constant. Again this deviation could be due to variation of  $D_{ps}Z$  with concentration. Therefore,  $K_{ps}Z\sqrt{D^2_{ps}Z}$  should be the real basis for deciding the rate controlling step. As table 4 indicates, variation of  $D_{ps}Z$  alone cannot account for the variation in  $K_{ps}Z$  completely. It is not possible to offer any concrete explanation at this stage, but some concentration dependent factors seems to be playing a role or there may be surface effects.

While comparing the results for experiments 5 and 6, it can be seen that mass transfer coefficient values in exp-5 has increased by a factor of 2 than in exp. 6,4, though lower turning velocity and higher residence time has been observed in the later case. The results in table 4 indicates the variation of diffusion coefficient due to change in aqueous medium.

that have contributed to the enhancement of the mass transfer coefficient values. In the case of experiment 7 and 8 with bigger drop size and in the same medium as in exps. 5 and 6, the mass transfer coefficient values has differed only by 22 percent, even though the diffusion coefficient values are very much different. Photographic studies as indicated earlier revealed that the bigger droplets oscillated vigorously during its passage through the aqueous phase and no droplet oscillation was there in the case of smaller one. Since the residence time and terminal velocity in exp. 7 and 8 had not differed much, it may be concluded that the droplet oscillation had influenced the mass transfer coefficient values.

#### D. Correlation of experimental data.

Saypolis number, drag coefficient, Schmidt number, Sherwood number have been calculated from the data in tables Ia, Ib and using average diffusion and mass transfer coefficient from experimental results. The values are given in table 3.

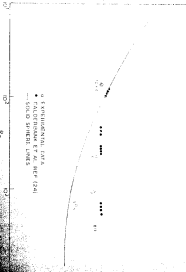
experimental drag coefficient values have been plotted against Reynolds number in log scale in fig.7 and compared with solid sphere behaviours. In the case of small drops in high viscosity fluids and in the range of Re below 100 as in the case of experiments 1-4, the deviation from solid sphere line is not much. This is in conformity with the photographic observations that small drops did not oscillate and thus behaved like solid spheres. In the case of experiments 5 and 9 with small droplets in water, the slight deviation from solid sphere line is there which indicated <sup>oscillation</sup> in the droplet. The point 8,7,8 matches with results of Calderbank<sup>14</sup> et al

TABLE 4

Calculated from table No. 1a, 1b  
and plots  $S_0$ ,  $S_0$

Exp. No.	average diffusion coeff. of $\text{Fe}^{2+}$ in $\text{cm}^2/\text{sec.}$	average mass transfer coeff. in $\text{cm}/\text{sec.}$	$S_0$	$C_1$	$S_{00}$	$S_{00}$
1	$4.87 \times 10^{-7}$	$1.88 \times 10^{-2}$	73.0	.931	$1.07 \times 10^3$	$5.12 \times 10^3$
2	$1.33 \times 10^{-7}$	$1.04 \times 10^{-2}$	75.0	.955	$7.58 \times 10^3$	$1.30 \times 10^4$
3	$7.72 \times 10^{-7}$	$2.39 \times 10^{-2}$	75.0	.970	$1.50 \times 10^5$	$6.95 \times 10^3$
4	$4.95 \times 10^{-7}$	$1.95 \times 10^{-2}$	73.0	.948	$2.07 \times 10^3$	$6.15 \times 10^3$
5	$5.07 \times 10^{-7}$	$1.44 \times 10^{-1}$	1250	.50	$1.03 \times 10^3$	$5.77 \times 10^3$
6	$2.76 \times 10^{-6}$	$8.7 \times 10^{-2}$	445	.805	$4.74 \times 10^3$	$1.33 \times 10^3$
7	$5.79 \times 10^{-6}$	$15.4 \times 10^{-2}$	1060	.815	$6.55 \times 10^3$	$10.55 \times 10^3$
8	$6.46 \times 10^{-6}$	$1.30 \times 10^{-1}$	2820	.882	$1.13 \times 10^3$	$6.79 \times 10^3$
9	$6.03 \times 10^{-6}$	$1.39 \times 10^{-1}$	1250	.83	$1.10 \times 10^3$	$3.64 \times 10^3$





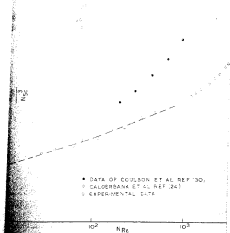


FIG. 8. CONTINUOUS PHASE MASS TRANSFER COEFFICIENT CORRELATION FROM AMALGAM DROP DATA

within the limits of experimental error. The logarithmic results revealed substantial oscillation in these systems.

Heat transfer from droplets to a continuous phase with two liquid system had been studied by Calderbank<sup>24</sup> and coworkers. The relationship obtained by them is presented in fig.4 along with those of Condon<sup>25</sup> et al. Calderbank<sup>24</sup> et al had a situation similar to present investigation in the sense that they employed falling secondary droplets in aqueous-alcohol mixture and studied the aqueous control case. Hence in the similar manner the experimental data of the present investigation have also been plotted in fig.5.

However, as figure 5 show, the data from this investigation are approximately an order of magnitude higher than those of Calderbank et al<sup>24</sup>. The results of Condon<sup>25</sup> et al deviate from the other and appears to merge with the present data when the former is extrapolated to higher Re values.

A comparison with heat transfer from solid spheres reveals that at low Reynolds no, oscillation inside the droplet does not have any appreciable effect on continuous phase mass-transfer coefficient. According to Calderbank et al, their data deviated from the solid sphere behaviour above  $Re \approx 100$  presumably due to droplet oscillation. If this interpretation is correct then it is to be noted that the droplet oscillation or air shear causes depending upon the system will result in the departure from solid sphere behaviour and may have entirely different effect on the mass-transfer coefficient. The higher positive departure of Condon's results cannot be otherwise explained. Following the same argument it may be said that perhaps the droplet oscillation began at much lower Re in the present

investigation because of large lowering of surface tension as a result of high mass transfer rates. Also a high mass transfer rate may by itself change the correlation.

or a --

# 7. CONCLUSIONS AND DISCUSSION

It is strongly felt that to plant increase the dehydrochlorination of molten metal over and above that it otherwise takes place to a large extent when metal droplets passed through the thick layer of slag. In order to study the possibilities of mass-transfer from two droplets a suitable system had been selected and the model was studied under most favourable conditions. All the experiments were conducted at 250° C. by passing refractory-silica analog droplets of different sizes through aqueous media having various concentration of glycerol and ferric ion. Ferric concentrations in aqueous phase were determined by polarographic technique, then by suitable stoichiometry the depletion of ferric ion in the aqueous media were obtained. By suitable relationship mass-transfer coefficients were calculated. Diffusion coefficient of ferric ion in the different aqueous media were measured, feeding velocity and residence time for the droplets in the aqueous phase were determined by photographic techniques.

The conclusions of the present investigations are summarized as follows:

1) appreciable amount of mass-transfer could not be measured even by polarography when the experiments were conducted at 250°C in the present apparatus. By increasing the column height, the residence time for the droplets in the aqueous phase could be increased and appreciable amount of mass-transfer could be measured at 250°C. With a short column, experiments at higher temperature solved the problem.

2) Systematic studies revealed that aqueous surface tension varied in all experiments.

3) Experiments with 70 wt per cent glycerol in aqueous phase revealed that the value of mass-transfer coefficients decreases progressively with increase in the concentration of ferric ion. This could be attributed to lowering of diffusion coefficient due to increase of ferric ion concentration.

4) In the case of small droplets, the mass-transfer coefficient decreased with increase in  $u$ - $v$  viscosity of the aqueous phase whereas with bigger droplets, the difference in the mass-transfer coefficient values were small because of severe droplet oscillation during their passage through the aqueous phase.

5) Smaller droplets behaved more or less as solid sphere while  $u$  or  $v$  along through high viscosity media, whereas in low viscosity media, oscillation to some extent could be observed. In the case of bigger droplets, severe oscillation in the different viscosity media had been observed.

6) Terminal velocity and residence time for all the droplets in the different aqueous media had been determined and systematic variations had been observed.

7) Photographic studies revealed that the smaller droplets were reaching their terminal velocity within 1 cm from the top of liquid surface where as 2-3.5 cm in the case of bigger ones.

8) The mass-transfer coefficients were one order magnitude higher than that expected from solid sphere behavior presumably because of droplet oscillations and possibly the Marangoni effect.

SYMBOLS

$\delta$	= area in $\text{cm}^2$
$\delta v$	= area of a sphere whose volume is equal to the volume of ellipsoid in $\text{cm}^2$ .
$C$	= concentration in g mole/l.
$C_0$	= concentration in the bulk
$D$	= diffusivity in $\text{cm}^2/\text{sec}$ .
$d_p$	= diameter of the drop in cm
$d_e$	= equivalent diameter in cm
$d_H$	= diameter in horizontal direction in cm.
$d_V$	= diameter in vertical direction in cm.
$e$	= eccentricity of drop $\frac{d_H}{d_V}$
$e^2$	= eccentricity of drop $\frac{d_H^2}{d_V^2}$
$g$	= gravitational acceleration $\text{cm/sec}^2$
$K_0$	= overall mass-transfer coefficient $\text{cm/sec}$ .
$k_D$	= drop phase mass-transfer coefficient $\text{cm/sec}$ .
$k_c$	= continuous phase mass-transfer coefficient
$V$	= terminal velocity $\text{cm/sec}$ .
$V_L$	= terminal velocity for liquid drop
$V_S$	= terminal velocity for solid sphere from Stokes law.
$r$	= radius of the droplet in cm
$Re_D$	= Reynolds number $\frac{\rho_0 V d_p}{\mu}$
$Re_C$	= critical number $Re \frac{\mu}{\rho V d_p}$

$\tau_{12}$  = average value  $\frac{\tau_{12}}{n}$

n = particles

# SYMBOLS

$\gamma$  = 0.1448

$\rho_0$  = density of continuous phase

$\rho_D$  = density for drop phase g./cc

$\sigma$  = surface tension dynes/cm

$\omega$  = frequency of oscillation per sec.

$\mu_0, \mu_D$  = continuous and drop phase viscosity in poise

$\delta$  = diffusion boundary layer thickness in cm.



REFERENCES

1. F.O. Kirkner, "Deep penetration affecting liquid interaction", in "Advances in Chemical Engineering", Vol 4 Edited by Don. C. et al. Academic Press.
2. V. Anshari, JNM. 1-2-3. 1966 2500, p-33
3. P. Deschamps, J of Chem. July 1969, p 68
4. J.C. Jochiel and P.Y. Chabert, Chem. Eng. Science vol 29, 1964 p 471.
5. S. Saito "Advances in Chemical Engineering" vol 4 p-73.
6. J.C. Jochiel et al. A.I.Ch.E. Journal vol 7, 1961, p. 794.
7. V.M. Loshak, "Physicochemical Hydrodynamics: Pressure Fall Interactions across in the Physical and Chemical Eng. Sciences.
8. Young and Kirkner, A.I.Ch.E. Journal vol 15, 1969 p 738.
9. C. Harwood et al. A.I.Ch.E. Journal July, 1970 p. 810.
10. F.S. Gesser and R.J. Haycock, Fuel April 1964, p 487.
11. R.H. Griffith, Chem. Eng. Sci. vol 13 1960, p 163.
12. I. Popadimitov et al, Chem. Eng. Sci. vol 24, 1968 p 899
13. I. Popadimitov, Canadian Journal of Chem. Eng. vol 47, 1969, p 42.
14. S. Gronig and F.O. Kirkner, Ibid ref. 10.
15. A.J. Hadden and S. Jones, A.I.Ch.E. Journal vol 3, 1957, p. 127.
16. Jones and Kirkner, A.I.Ch.E. Journal vol 18, 1966, p 430.
17. Angelo and Lightfoot, A.I.Ch.E. Journal, 1966, p 791.
18. Ky and Lightfoot, A.I.Ch.E. Journal vol 14, 1968, p 830.
19. H. Chen, A. Yoshizawa and K. Tate, "International Conference on the Science and Technology of Iron and Steel, Conference programs held in 1970, Sponsored by I.I.I.I.

22. K. Inoki, A. Kikuchi and T. Koshi, *ibid.*, *loc. cit.*
23. L. J. Fetters, *J. Polymer Sci. A*, **1**, 1, 1, 1963, p. 1.
24. J. L. Fetters, *J. Polymer Sci. A*, **1**, 1, 1963, p. 1.
25. J. L. Fetters and J. L. Fetters, *J. Polymer Sci. A*, **1**, 1, 1963, p. 1.
26. J. L. Fetters and J. L. Fetters, *J. Polymer Sci. A*, **1**, 1, 1963, p. 1.
27. J. L. Fetters and J. L. Fetters, "The Transfer of Energy to Polymer Chains", *J. Polymer Sci. A*, **1**, 1, 1963, p. 1.
28. J. L. Fetters and J. L. Fetters, "The Transfer of Energy to Polymer Chains", *J. Polymer Sci. A*, **1**, 1, 1963, p. 1.
29. J. L. Fetters and J. L. Fetters, "The Transfer of Energy to Polymer Chains", *J. Polymer Sci. A*, **1**, 1, 1963, p. 1.
30. J. L. Fetters and J. L. Fetters, "The Transfer of Energy to Polymer Chains", *J. Polymer Sci. A*, **1**, 1, 1963, p. 1.

100

These results in the two experiments are in excellent agreement with the theoretical predictions.

[illegible]

ME-1971-M-CHA-MAS